

Article

Crystal-Chemical and Spectroscopic Study of Gem Sphalerite from Banská Štiavnica, Slovakia

Peter Bačík ^{1,2,*}, Jana Fridrichová ¹, Olena Rybnikova ¹, Ján Štubňa ³, Ľudmila Illášová ³, Radek Škoda ⁴, Tomáš Vaculovič ⁵, Zuzana Pulišová ³ and Peter Sečkář ¹

¹ Department of Mineralogy, Petrology and Economic Geology, Faculty of Natural Sciences, Comenius University in Bratislava, Ilkovičova 6, SK-842 15 Bratislava, Slovakia

² Earth Science Institute, Slovak Academy of Sciences, Dúbravská cesta 9, SK-845 28 Bratislava, Slovakia

³ Gemmological Laboratory, Department of Geography and Regional Development, Faculty of Natural Sciences, Constantine the Philosopher University in Nitra, Nábřežie mládeže 91, 94974 Nitra, Slovakia

⁴ Department of Geological Sciences, Masaryk University, Kotlářská 2, 61137 Brno, Czech Republic

⁵ Department of Chemistry, Masaryk University, Kamenice 5, 62500 Brno, Czech Republic

* Correspondence: peter.bacik@uniba.sk

Abstract: A complex crystal-chemical investigation based on spectroscopic methods, Electron MicroProbe Analysis (EMPA), and Laser Ablation Inductively Coupled Plasma Mass Spectrometry (LA-ICP-MS) was made on sphalerite samples from the Terézia and Rozália veins in the Banská Štiavnica ore district. The yellow (sample A) and olive-green sphalerite (C) are in association only with quartz; orange sphalerite (B) is associated with quartz and chalcopyrite; and black sphalerite (D) is associated with galena, chalcopyrite, quartz, and baryte. EMPA revealed that Cd and Fe are substituting for Zn with variable proportions; the Cd/Fe ratio decreases from 2.82–2.85 in the A sample to 0.42 in the D sample. LA-ICP-MS showed that, except Cd and Fe, only Mn has content above 20; Co and Cu vary between 2 and 17 ppm. The optical absorption spectra exhibit absorption between 644 and 740 nm with three smaller humps at 669–671, 698–702, and 732–743 nm, and weaker absorption bands at 858–894 nm in the NIR region, which can be all assigned to crystal-field transitions of Fe²⁺. The absorption edge starts at about 600 nm to the UV region. Minimal absorption is in the yellow-red part of the visible spectrum giving rise to yellowish-orange and orange-red colors. Absorption in the red region for olive-green sphalerite is more pronounced, explaining the shift to greenish hues. In black sphalerite, the absorption pattern is similar to the olive-green sphalerite, but the bands in the 644 to 740 nm region are less defined. The black color could be caused by slightly higher concentrations of Fe, the smaller size of individual crystals in the aggregate reducing macroscopic transparency, and/or the presence of submicroscopic inclusions.

Keywords: sphalerite; cleiophane; crystal chemistry; Raman spectroscopy; optical absorption spectroscopy; gemology; Banská Štiavnica; Slovakia



Citation: Bačík, P.; Fridrichová, J.; Rybnikova, O.; Štubňa, J.; Illášová, L.; Škoda, R.; Vaculovič, T.; Pulišová, Z.; Sečkář, P. Crystal-Chemical and Spectroscopic Study of Gem Sphalerite from Banská Štiavnica, Slovakia. *Minerals* **2023**, *13*, 109. <https://doi.org/10.3390/min13010109>

Academic Editors: Andy H. Shen, Chaowen Wang and Bo Xu

Received: 1 December 2022

Revised: 3 January 2023

Accepted: 7 January 2023

Published: 10 January 2023



Copyright: © 2023 by the authors. Licensee MDPI, Basel, Switzerland. This article is an open access article distributed under the terms and conditions of the Creative Commons Attribution (CC BY) license (<https://creativecommons.org/licenses/by/4.0/>).

1. Introduction

Sphalerite is not a common gemstone; it is most often used as zinc and cadmium ore and is also the main carrier of gallium, germanium, and indium [1]. Usually, it is dark brown to black. When it is transparent or translucent and has an attractive color—yellow-brown, red-brown, green, yellow, or orange—it is suitable for faceting, especially for collectors. It is not commonly used in jewelry because it has a low hardness (3.5–4 Mohs scale) and good cleavage [2]. Therefore, for jewelry purposes, it is set mainly to pendants or brooches, and it is not suitable for rings. Sphalerite has several varieties—the abundant black marmatite, cleiophane, which is colorless to white and translucent; red sphalerite called přibramite, a white collomorphic brunckite variety [3]; and schalenblende—colloform, layered sphalerite [4].

Gemological laboratories report sphalerite quality and clarity from VVS to I3 and color from greenish to dark brown-orange (according to RGB codes, the international color is expressed as 068—green, 050—yellow, 040—light orange-yellow, 025—medium orange-yellow, and 028—medium dark red-orange, strong). The large cut crystals can weigh up to 55 ct. The most common piece sizes are up to 3 ct; quite often, there are sizes of 10 to 20 ct [5]. Sphalerites are usually cut into facet cuts and cabochons. The international color scale does not consider black sphalerites as gemstones.

Cut sphalerites are more common in Mexico (Tres Marias), USA (New York, Colorado), Spain (the Aliva mines), and Bulgaria (Madan ore field) at the gemstone market [1,6–8]. The most famous gem-quality sphalerite is from the Aliva mine, Santander, Spain, where large transparent red-orange gem-quality specimens are reported [6]. Another valuable source of gemmy sphalerites is in Cananea, Sonora, Mexico, where fine green, transparent, often pale-colored and color-zoned material is observed. Exceptional sphalerite crystals up to 8 cm in size are reported [9,10]. Numerous localities are described in the United States, e.g., the Iron Cap mine, Aravaipa District, Graham County, or the Westinghouse mine at Duquesne, Santa Cruz County [9]. Good specimens were also described in Colorado [8,9]. Transparent sphalerites are also known from Pb-Zn ore deposits of the Madan ore district, Bulgaria [11–13]. Exceptional gem-quality sphalerites are reported from Mont Saint-Hilaire, Quebec, Canada [5]. Sphalerites of yellow-green, brownish-green, and dark-red colors, perfectly transparent, with weight up to 55 ct in the faceted state, are reported there. Gem-quality sphalerites are documented in Kipushi, Democratic Republic of the Congo [1]. Green sphalerite is also described from Steinperf, Germany [14].

Sphalerites are rarely studied in detail from a gemological perspective. Gem-quality samples from the USA and Canada were characterized from a historical and geological point of view [5,7–9]. Most of the papers are focused on the metallogenic potential of sphalerites [1,11,13,15–17], rather than its gemological application. Major elements and trace elements composition are reported from skarn at Baisoara (Romania), Toyoha (Japan), Tres Marias (Mexico), and numerous localities from China studied with the help of LA-ICP-MS and EPMA [1,15–17]. The crystal morphology of fluid inclusions is thoroughly studied in sphalerites of the Madan ore district, Bulgaria [11]. Optical absorption spectroscopy examination of sphalerite crystals is reported from Steinperf, Dill Syncline, Germany and from Santander, Spain [14,18–20]. Raman spectra of sphalerite of variable quality are reported by [21–25]. There is a lack of modern comprehensive research on gem-quality sphalerite that combines all the methods and interprets them in order to find dependencies from each other. The current research attempts to combine the methods and provide a complex description of different colors of gem-quality sphalerites.

Sphalerite from Banská Štiavnica, mostly cleiophane variety, has optical properties (color, transparency) which make it useful as the gemological material comparable with the other famous sphalerite gem deposits. The aim of this study is the complex crystal-chemical investigation of sphalerite from the Terézia (cleiophane variety) and Rozália (marmatite variety) veins in the Banská Štiavnica ore district based on spectroscopic methods, Electron MicroProbe Analysis (EMPA), and Laser Ablation Inductively Coupled Plasma Mass Spectrometry (LA-ICP-MS).

2. History of Mining and Sphalerite Occurrences in Banská Štiavnica

Banská Štiavnica is one of the world's most important historical mining sites, which belongs to a UNESCO cultural heritage. The first settlement dates back to 3000 BC when the Celts began to establish the first mining communities that were taken over by the Slavs in the fifth to sixth centuries. The first written mention of the “mining town” dates back to 1156, but the first real evidence was dated in 1217 when the area was called “Bana” and later, in 1228, was renamed to Strieborné Bane (Silver Mines). During the 12th and 13th centuries, the area was colonized by the Germans. In 1255, the name Schebnyzbana appeared, which was Germanized in 1275 to Schemnitz; the Slovak versions of the name—Sczawnica and

Stawnicza—first appeared in 1449 and 1713. Since medieval times, it was part of the Austrian Empire. The name Banská Štiavnica finally settled in 1920 [26].

Banská Štiavnica became famous mainly for silver and gold mining. Silver mining culminated in the 18th century when Banská Štiavnica was one of the largest cities in the monarchy. In the 20th century, mainly lead, zinc, and copper ores were mined. The main mining in Banská Štiavnica ended in 1993. At present, only the Rozália mine in the Hodruša-Hámre is open, which is the only active gold mine in Central Europe [26].

Sphalerite is one of the most common minerals in the Banská Štiavnica district. Its crystals are usually black, brown, or yellow-brown; yellow, dark green, and green-black crystals can be also found, but pale green and colorless ones are very rare. Rounded, yellow-brown crystals up to 5 cm are characteristic of Banská Štiavnica sphalerites; the abundant tetrahedral specimens from Hodruša are black [26]. During history, more sphalerite occurrences were found in the Terézia shaft (Figure 1) [27]. The green and brown, translucent to opaque, dodecahedral to octahedral crystals came from the Pacher adit; and the dark brown to black tetrahedral crystals were from the Michal mine, the Terézia mine, the Brenner adit, and the Pacher adit, which were associated with galena, pyrite, chalcopyrite, and quartz. Some tetrahedral to octahedral sphalerite crystals are spinel-law twins. Rounded crystals, yellow to yellow-brown, up to 2.5 cm, were discovered in 1989–1990 between the fifth and ninth Nová shaft levels. Large crystals were also located in the Amália vein. Green to dark green sphalerites were found in Štiavnické Bane and the Göllner adit, Terézia vein. The largest crystals were 4 cm in size. Attractive black glossy sphalerite druses associated with galena and chalcopyrite occurred in the Amália vein and on the 14th and the 18th level of the Rozália mine, Hodruša-Hámre, where they were discovered in 1995 and 2000 [26,28].

3. Geological Setting

The Banská Štiavnica ore deposits are centered on the largest stratovolcano in the Central Slovakia Neogene Volcanic Field, in the Inner Western Carpathians, with an area of over 2000 km² (Figure 1). This stratovolcano began to form about 15 million years ago (15 Ma); the complex formation process was marked by intervals of igneous extrusions, subsidence, and weathering, with frequent subsurface intrusions by igneous stocks and the formation of epithermal veins. The volcano development was accompanied by metallogenetic processes that produced precious metals and polymetallic mineralization. This mineralization conditioned the development of mining cities (Banská Hodruša, Banská Štiavnica) and consolidated the mining tradition [29].

The development of the Štiavnica stratovolcano can be divided into five stages. Stage 1: The lower stratovolcanic structure development (Early to mid-Badenian) during the explosive–effusive to intrusive activity was formed by an extensive andesite stratovolcano, which forms the lower stratovolcanic structure. Stage 2: The depression development with marsh sedimentation in the top part of a stratovolcano. The depression development was formed due to the caldera subsidization, which was not accompanied by more severe volcanism manifestations. Stage 3: The Štiavnica caldera formation was conditioned by continued subsidization of the stratovolcano top part where the explosive–effusive and extrusive biotite-amphibolic andesites to the andesites–dacites activity of the Studená formation took place. Stage 4: The stratovolcano superstructure development was renewed by several eruptive activities in Sarmatian. Stage 5: Rhyolitic volcanism and Hodruša–Štiavnica horst development (Late Sarmatian to Pannonian). At this stage, rhyolite volcanism is evident, which has allowed the rhyolite magma to reach the surface by extensive fault systems [29].

Significant precious metal and polymetallic ores bodies and several mineralizations were created in the Štiavnica extensive stratovolcano. Sphalerite can be found at various stages of stratovolcano mineralization. Mineralization was developed in three stages: 1. The pre-ore-bearing stage formed in granodiorite with pyrite, epidote, albite, quartz, and carbonate; 2. The ore-bearing stage with dominant sphalerite and galenite (minerals dominate in this type of stratovolcano mineralization), a small amount of pyrite, chalcopyrite, linked

to quartz-epidote veins; 3. The ore-bearing stage with chalcopyrite, galenite, sphalerite, accessory tetrahedrite, gold, hematite, chalcocine, and bornite. High-temperature epithermal Au mineralization occurred in the pre-caldera stage of stratovolcano development, probably in close proximity to granodiorite intrusion. The sphalerite occurrence in this mineralization can be attributed mostly to the banded veins with the mineral association: quartz, orthoclase var. adular, rhodonite, rhodochrosite, Mn-calcite, pyrite, galenite, chalcopyrite, and gold. It may also occur in the Rozália vein and other epithermal veins in the mineral association: quartz, Fe/Ca carbonates, pyrite, galenite, chalcopyrite, tetrahedrite, polybase, hessite, and gold. Polymetallic epithermal vein mineralization of the Štiavnica type has a large vertical extent, uniform periods of silicified and sericitized zones development with a dominant polymetallic character with major minerals such as chalcopyrite, galenite, sphalerite, Ag sulfosalts, and gold in quartz-carbonate veins. Sporadic sphalerite occurrence with chalcopyrite, galenite, and marcasite can be identified in the precious metal mineralization, which is similar to the Carlin-type mineralization [30,31].

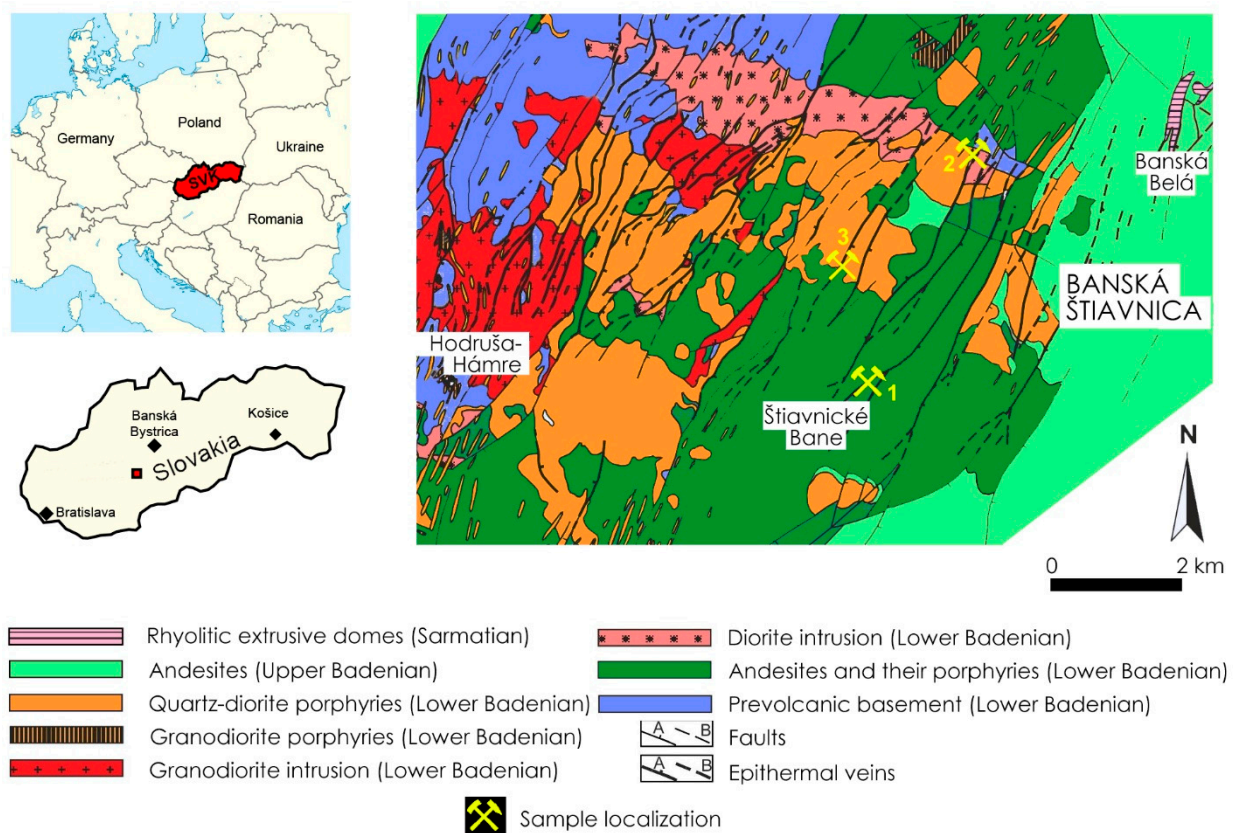


Figure 1. Geological sketch map of the Banská Štiavnica area (adapted, based on [31]) with sample localization: 1—Göllner adit, 2—Michal shaft, 3—Rozália mine.

4. Analytical Methods

The chemical composition of sphalerite was measured using a Cameca SX100 electron microprobe (Cameca company, part of Ametek group, Gennevilliers Cedex, France) operated in wavelength-dispersion mode at the Masaryk University, Brno, Czech Republic, under the following conditions: accelerating voltage 15 kV, beam current 20 nA, and beam diameter 5 μ m. The samples were analyzed with the following standards: ZnS (Zn $K\alpha$), FeS₂ (Fe $K\alpha$, S $K\alpha$), metallic Mn (Mn $K\alpha$), metallic Co (Co $K\alpha$), pararammelsbergite (Ni $K\alpha$, As $L\beta$), metallic Cu (Cu $K\alpha$), PbSe (Pb $M\beta$, Se $L\beta$), metallic Cd (Cd $L\beta$), InAs (In $L\alpha$), metallic Ag (Ag $L\alpha$), metallic Bi (Bi $M\beta$), and metallic Ge (Ge $L\alpha$). Detection limits of the measured elements varied between 150–400 ppm except for Ge (600–620 ppm), Cd (790–840 ppm), Ag (1150–1250 ppm), Zn (0.26–0.27 ppm), and Bi (2000–2200 ppm). From the measured

elements, only Zn, S, Fe, and Cd were above their respective detection limits; Ag, As, Bi, Co, Cu, Ge, In, and Mn were always below the detection limit. Analytical times were 15 to 40 s during measurement, depending on the expected concentration of the element in the mineral phase. Major elements were measured using shorter times, whereas longer times were applied for elements with a low concentration. The sphalerite chemical formula was calculated based on 2 atoms.

Instrumentation for Laser Ablation Inductively Coupled Plasma Mass Spectrometry (LA-ICP-MS) at the Department of Chemistry, Masaryk University, Brno, consists of a UP 213 laser ablation system (NewWave Research, Inc., Fremont, CA, USA) and Agilent 7500 CE ICP-MS spectrometer (Agilent Technologies, Santa Clara, CA, USA). A commercial Q-switched Nd-YAG laser ablation device worked at the 5th harmonic frequency corresponding to 213 nm wavelength. The ablation device was equipped with a programmable XYZ-stage to move the sample along a programmed trajectory during ablation. Target visual inspection and photographic documentation were achieved by the built-in microscope/CCD-camera system. A sample was enclosed in the SuperCell and was ablated by the laser beam, which was focused onto the sample surface through a quartz window. The ablation cell was flushed with a helium carrier gas which transported the laser-induced aerosol to the inductively coupled plasma (1 Lmin^{-1}). Sample argon gas flow was admixed with the helium carrier gas flow after the laser ablation cell to 1.6 Lmin^{-1} total gas flow. NIST SRM 610 silicate glass reference material was used to optimize the gas flow rates, the sampling depth, and MS electrostatic lens voltage in LA-ICP-MS conditions. This provided a maximum signal-to-noise ratio and minimum oxide formation (ThO^+/Th^+ count ratio 0.2%, U^+/Th^+ counts ratio 1.1%). Laser ablation required a 100 m laser spot diameter, 8 Jcm^{-2} laser fluence, and a 20 Hz repetition rate. The fixed sample position during laser ablation enabled 60 s hole-drilling duration for each spot. From the measured elements, Li, B, Mg, Al, Si, P, K, Ca, Cr, Ni, Rb, Sr, Y, Sn, Ba, La, Ce, Pr, Nd, Sm, Eu, Gd, Tb, Dy, Ho, Er, Tm, Yb, Lu, Hf, Hg, Th, and U were always below their detection limits.

Raman analyses were performed on the LabRAM-HR Evolution (Horiba, Jobin-Yvon, Kyoto, Japan) spectrometer system with a Peltier-cooled CCD detector and Olympus BX-41 microscope (Department of Geological Sciences, Masaryk University). Raman spectra excited by blue diode laser (473 nm) in the range of $50\text{--}4000 \text{ cm}^{-1}$ were collected from each stone using $50\times$ objectives. The acquisition time of 10 s per frame and 2 accumulations were used to improve the signal-to-noise ratio.

Optical absorption spectra of cut stones in the region (500–1000 nm) were measured with the GL Gem SpectrometerTM (Gemlab Group, Vancouver, Canada) with GL Halogen light source (10 W) at room temperature at the Department of Mineralogy, Petrology, and Economic Geology, Comenius University in Bratislava.

Both Raman and UV/Vis/NIR spectra of all samples were processed in Seasolve PeakFit 4.1.12 software. Raman and absorption bands were fitted to obtain exact band positions and deconvolute overlapping bands by the Lorentz function with variable width, automatic background correction, and Savitsky–Golay smoothing. Band fitting was gradually refined until it produced reproducible results with a square regression coefficient greater than 0.995.

5. Results

Four pieces of transparent, translucent, and opaque sphalerite var. cleiophane and marmatite were separated from the host rock. Two of them (from samples A and B) with the best gemological quality were faceted into round brilliant cuts with dimensions of $2.80 \text{ mm} \times 2.80 \text{ mm} \times 1.64 \text{ mm}$ (0.11 carat) and $1.71 \text{ mm} \times 1.74 \text{ mm} \times 1.14 \text{ mm}$ (0.025 carats). The gemological properties of cut stones are described in [32].

The yellow (sample A) and olive-green sphalerite (sample C) from the Göllner mine on the Terézia vein in Štiavnické Bane near Banská Štiavnica are in association only with quartz (Figure 2a,c). Sphalerite forms monocrystals and aggregates of a few crystals up to 12 mm. Orange sphalerite (sample B) from the 12th horizon of the Michal shaft, the Juraj

field on the Terézia vein in Banská Štiavnica is associated with quartz and chalcopyrite and forms larger crystals up to 20 mm (Figure 2a–c). The most typical morphologic shapes are cut tetrahedra. Black sphalerite from the Rozália mine in Hodruša-Hámre (Figure 2d) used for comparison as a gemologically uninteresting sample forms aggregates and polycrystals in a more varied association with galena, chalcopyrite, quartz, and baryte.



Figure 2. Studied samples of sphalerite: (a) yellow sphalerite from the Göllner mine on the Terézia vein in Štiavnické Bane near Banská Štiavnica (sample A); (b) orange sphalerite from the 12th horizon of the Michal shaft, the Juraj field on the Terézia vein (sample B); (c) olive-green sphalerite from the Göllner mine on the Terézia vein in Štiavnické Bane near Banská Štiavnica (sample C); (d) black sphalerite from the Rozália mine in Hodruša-Hámre (sample D).

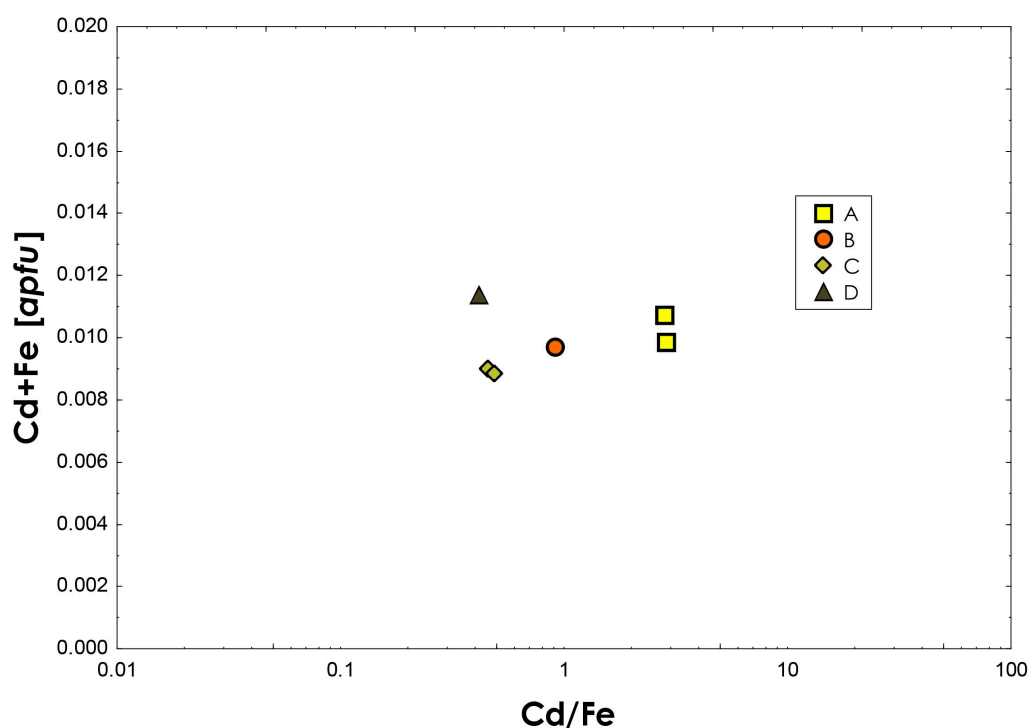
5.1. Chemical Composition

Electron microprobe analysis was made on all four types of sphalerite. It revealed that Cd^{2+} and Fe^{2+} are the most abundant cations substituting for Zn^{2+} in all studied samples but with variable proportions (Table 1). All other elements were below their respective detection limits on EMPA in all studied samples. Although the sum of Cd^{2+} and Fe^{2+} is relatively constant between 0.009 and 0.011 apfu (atoms per formula unit), there are significant differences among the individual samples. The $\text{Cd}^{2+}/\text{Fe}^{2+}$ ratio decreases from 2.82–2.85 in the yellow A sample to 0.42 in the black D sample (Table 1, Figure 3).

Since the majority of elements in the studied samples were below the EMPA detection limit, two cut samples (A and B) were analyzed with LA-ICP-MS (Table 2). This revealed that along with the most abundant Cd and Fe, only Mn has content above 20, and in the A sample, it attains 100 ppm. Cobalt and copper vary between 5 and 17 ppm and between 2 and 9 ppm, respectively. In some spots, Ga and Pb exceed 1 ppm. Ag is constantly present but below 1 ppm. No light elements between Li and F were observed.

Table 1. Electron microprobe analyses of sphalerite samples, first presented in wt% (standard deviation on the second decimal place in brackets) and then in apfu, calculated based on 2 atoms.

	Sf-A	Sf-A	Sf-B	Sf-C	Sf-C	Sf-D
Cd	0.91 (9)	0.84 (9)	0.54 (8)	0.33 (8)	0.34 (8)	0.39 (8)
Fe	0.16 (2)	0.15 (2)	0.29 (2)	0.35 (2)	0.34 (2)	0.46 (2)
S	32.72 (24)	33.00 (24)	33.44 (24)	33.11 (24)	33.19 (24)	33.14 (24)
Zn	65.86 (26)	66.10 (27)	65.78 (27)	66.13 (27)	66.22 (27)	65.89 (27)
Total	99.76	100.15	100.12	100.08	100.13	99.89
Cd²⁺	0.008	0.007	0.005	0.003	0.003	0.003
Fe²⁺	0.003	0.003	0.005	0.006	0.006	0.008
Zn²⁺	0.987	0.986	0.977	0.984	0.984	0.981
S²⁻	1.001	1.004	1.013	1.005	1.006	1.007
Cd²⁺/Fe²⁺	2.819	2.855	0.914	0.460	0.487	0.416

**Figure 3.** The Cd²⁺/Fe²⁺ vs. Cd²⁺+Fe²⁺ plot with data from EMPA analyses of each sample.**Table 2.** LA-ICP-MS analyses of studied sphalerite; d.l.—detection limit.

	Na	Sc	Ti	V	Cr	Mn	Fe	Co	Cu	Ga	Ge	Zr	Ag	Cd	In	Sb	Pb
A	<	0.14	0.32	<	<	83.54	2934	14.69	3.30	0.67	1.11	<	0.78	7996	0.04	0.66	0.24
A	<	<	0.33	<	<	100.29	3056	16.82	1.98	0.80	<	<	0.91	10,130	0.04	0.65	1.20
A	<	<	<	<	<	83.50	3152	12.15	6.82	4.30	<	0.10	0.58	9059	0.03	0.35	0.43
B	25	<	<	<	<	20.18	3516	8.11	3.08	0.58	<	0.13	0.23	6708	1.06	0.21	<
B	29	<	<	<	<	24.66	4348	5.60	8.61	5.03	<	0.14	0.94	5918	0.74	<	0.06
B	33	<	0.34	0.14	1.81	24.63	4312	7.82	8.57	2.22	<	0.67	0.56	7368	0.15	<	<
d.l.	23	0.12	0.05	0.10	0.70	0.34	1	0.05	0.09	0.05	0.79	0.05	0.05	1	0.03	0.05	0.05

5.2. Spectroscopic Data

Raman spectroscopy was accomplished on all sphalerite samples (Figure 4; Table 3). Raman spectra are a little bit different in some vibrations, depending on the sample. We can distinguish two optic phonons, i.e., longitudinal-optic (LO) and transverse-optic

(TO), according to [21], and three optic phonons, i.e., LO—longitudinal optical mode, TO—transverse optical mode, LA—longitudinal acoustic mode; two phonons denote that two phonons are involved in the transition according to [22]. The first-order Raman spectra of sphalerite showed the LO and TO modes at 348–349 and 271–273 cm^{-1} [23,24]. The second-order Raman spectra, which can be assigned to LA at 88 and 110 cm^{-1} [24], are completely missing in the studied samples.

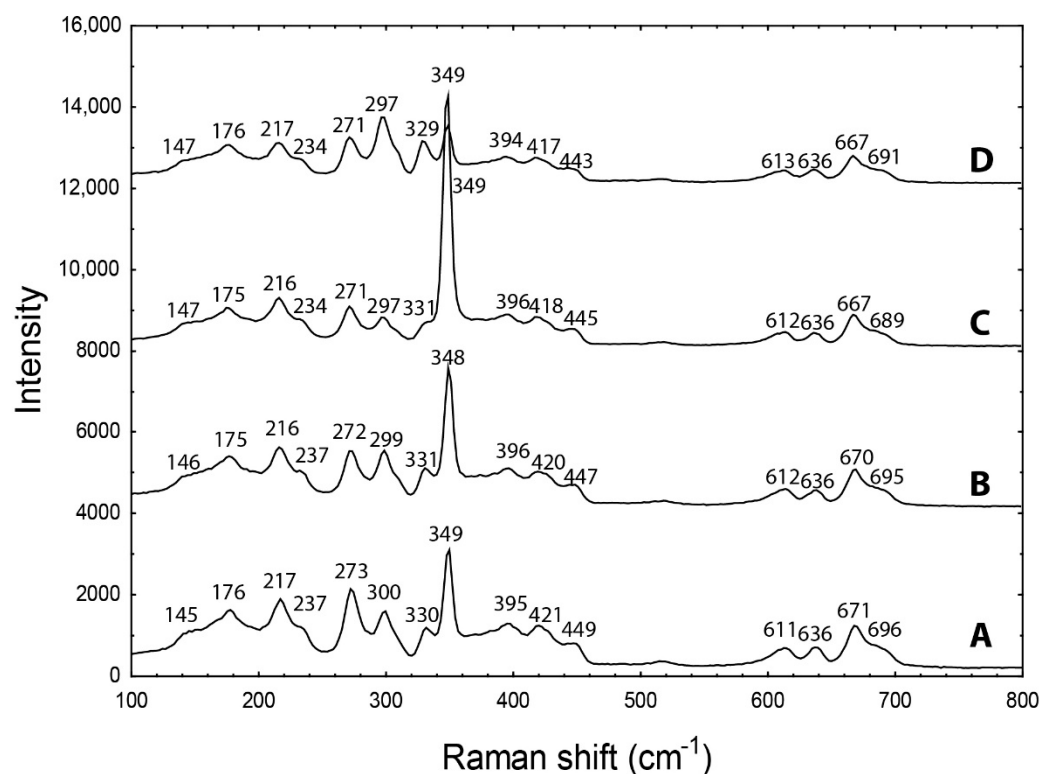


Figure 4. Raman spectra of studied sphalerite samples.

Table 3. Assignment of Raman bands in the studied sphalerite samples [21–24].

Assignment	A	B	C	D
Lattice vibrations	145	146	147	147
TA overtone	176	175	175	176
LA overtone	217	216	216	215
	237	237	234	234
TO	273	272	271	271
Fe-S	300	299	297	297
Fe-S	330	331	325	329
Cd-S	349	349	348	349
TO+TA	395	396	396	394
TO+LA	421	420	418	417
LO+LA	449	447	445	443
TO2 phonon	611	612	612	613
LO+TO	636	636	636	636
LO2 phonon	671	670	667	667
	696	695	689	691

The optical absorption spectra of studied sphalerites were taken between 500 (20,000 cm^{-1}) and 1000 nm (10,000 cm^{-1}) (Figure 5). The spectra exhibit strong absorption at about 644 (15,527 cm^{-1}) to 740 nm (13,513 cm^{-1}) with three smaller humps at 669, 702, and 733 nm (14,947, 14,245, 13,642 cm^{-1}) with deviation 2–11 nm from each other. Weaker absorption is

observed in the NIR region at about 858 and 894 nm ($11,655$ and $11,185$ cm^{-1}). The overall absorption increase towards the UV region starts at about 600 nm ($16,666$ cm^{-1}).

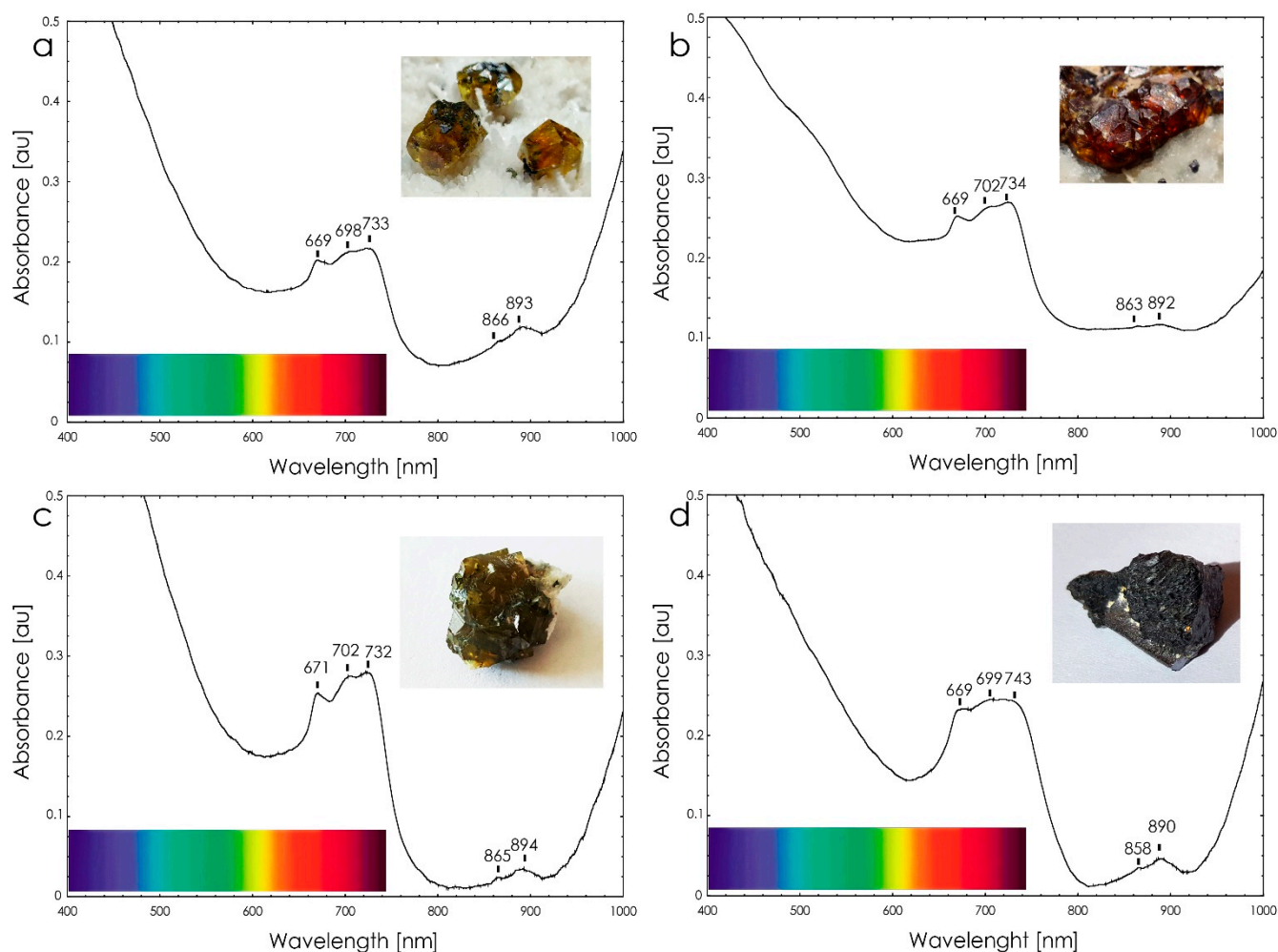


Figure 5. Optical spectra of studied sphalerite samples: (a) yellow sphalerite—sample A; (b) orange sphalerite—sample B; (c) olive-green sphalerite—sample C; (d) black sphalerite—sample D.

Minimum absorption is in the yellow, orange-red part of the visible spectrum giving rise to the crystals' yellowish-orange and orange-red color (Figure 5a,b). On the other hand, absorption in the red region for olive-green sphalerite (Figure 5c) is more pronounced compared to yellowish-orange and orangy-red sphalerites, explaining the shift of the color to greenish hues. In the case of black sphalerite, the absorption pattern is similar to the olive-green sphalerite; however, the bands in the 644 ($15,527$ cm^{-1}) to 740 nm ($13,513$ cm^{-1}) region are less defined, creating one wide band (Figure 5d).

A broad absorption band in the region from 644 ($15,527$ cm^{-1}) to 740 nm ($13,513$ cm^{-1}) could correspond to crystal-field bands of Co and Fe together, while bands 858 and 894 nm ($11,655$ and $11,185$ cm^{-1}) in the NIR region correspond to Fe only [25].

6. Discussion

The sphalerite crystal structure can accommodate a large variety of elements; the most significant of them are Fe and Cd. The Cd concentration can attain sufficient values for sphalerite being used as Cd; e.g., giant Zn–Pb deposits such as Red Dog (Alaska) are economically exploited for this element [1]. Trace elements in sphalerite can use simple substitution of similar-sized ions with the same charge ($\text{Zn}^{2+} \leftrightarrow \text{Fe}^{2+}$, Cd^{2+} , Mn^{2+} , Co^{2+} or $\text{S}^{2-} \leftrightarrow \text{Se}^{2-}$) or coupled substitution of ions with different charges (e.g., $2 \text{Zn}^{2+} \leftrightarrow \text{Cu}^{+} + \text{In}^{3+}$) [1,15]. Substitution mechanisms for other elements commonly found in sphalerite (e.g., Sn, Ag,

Ga, and Ge) remain less well constrained, and it is not clear for elements such as Pb, Tl, As, Sb, and Bi whether they might enter the sphalerite structure or are almost always present as mineral inclusions [15]. The limits for entering the sphalerite structure can be derived from the formal charge of cations (e.g., four-valent cations) and ionic radii (e.g., Fe^{3+} has a too-small ionic radius of 0.49 Å [33], Ag^+ a too-large radius with 1 Å [33]). However, electronegativity has to be also considered; Zn has 1.65, Cd 1.69, Fe 1.83, but Ag 1.93 and Cu 1.90. Therefore, although elements possibly substituting for Zn can be abundant in the environment, they can prefer different minerals.

The LA-ICP-MS analysis revealed that studied samples of sphalerite from Banská Štiavnica and Hodruša-Hámre are relatively poor in trace elements except for Fe, Cd, and partly also Mn. However, Mn content is lower by two to three orders compared to Fe and Cd. Other elements (In, Sb, Co, Cu, Ga, Ag, Pb) are scarce.

The Fe content in studied sphalerite is relatively low compared to other world localities. It is significantly lower than in most of the skarn and stratabound deposits, but it shares similarities with some sphalerite from Neogene epithermal mineralization in Romania [1]. However, Romanian sphalerite is significantly richer in Cu and Mn [1] than the studied samples. The Fe proportion in studied samples can be correlated with the position of sphalerite within the mineralization and its spatial position. Studied sample A is from the shallower, almost surface part of the Terézia vein, and it has lower Fe than sample B from a deeper part of the same vein—the 12th horizon of the Michal shaft. The D sample from Hodruša-Hámre with the highest Fe content is also from the deeper parts of the Rozália mine.

Sphalerite from Slovakia can be considered relatively rich in cadmium. Sphalerites from Neogene epithermal mineralization in Romania and also from stratabound deposits contain 1000–7700 ppm [1]. Sphalerites from skarns are typically uniform within the 2500–10,800 ppm range except with the exception of the Baisoara skarn deposit (Romania), where cadmium concentration shows up to 73,800 ppm [1]. Measured concentrations of Cd in gem-quality sphalerite from Slovakia range from 5917 and 10,130 ppm. Cadmium is typically higher in lower-temperature deposits [15,16], which explains its opposing relationship with Fe in the studied samples.

Based on the Mn vs. Fe (Figure 6a) and Cd/Fe vs. Mn (Figure 6b) ratios, studied sphalerites fall into the field of Mississippi Valley-Type (MVT) deposits [17]. However, although MVT sphalerite is characterized by low Fe, Mn, In, and Co, and high Ge, Cd, and Ga contents [1,15,17], studied samples are low in Ge and Ga. In contrast, sphalerite from most magmatic-related deposits is characterized by high Fe, In, Mn, and Co, but low Ge and Cd contents [1,15], so it also cannot be used to discriminate the genetical origin of samples and its influence on their chemical composition. The Zn/Cd ratio could also discriminate sphalerite from various genetic types of deposits. Volcano-sedimentary and Alpine (MVT)-type deposits have the highest Zn/Cd ratios of 417 to 531 [34]. However, studied sphalerite samples have Zn/Cd ratios of 97–166, which is significantly lower. In contrast, it is typical for hydrothermal deposits, including vein magmatic-related and skarn deposits, with the Zn/Cd ratios between 104 and 214 [34]. Consequently, we can assume that the most important factor for the generally low trace-element content, except for Cd, is the low temperature of source fluids in the hydrothermal veins. This low trace-element composition resulted in the exquisite optical properties of studied sphalerite.

Sphalerite can have quite a large variety of colors. A dark black color is commonly explained by high Fe content (>6 wt.%) [1]. However, when iron concentration is low, other elements can also be highly influential on color. According to [35], the yellow colors of sphalerite may be caused by Ge, Cu, and Hg; reddish by Ce, Sn, and Ag; and green colors by Co and Fe. Furthermore, gem-quality green sphalerite from Congo has Co content in the range of 20 to 820 ppm and Cu [36].

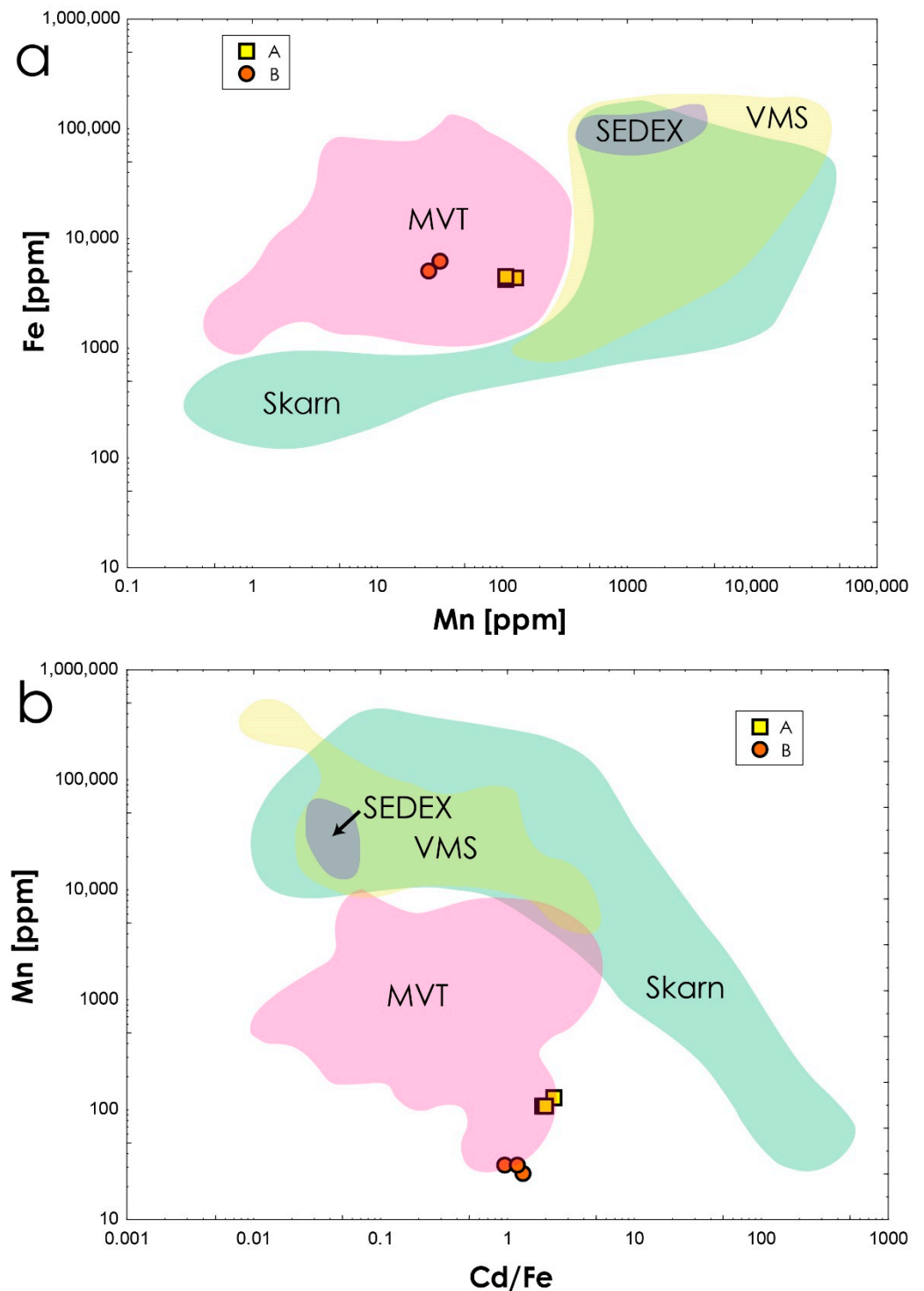


Figure 6. Plots of (a) Mn vs. Fe and (b) Cd/Fe vs. Mn in studied sphalerite samples based on the LA-ICP-MS data. Fields for selected genetic types are from [28].

Iron and cobalt are primary elements creating absorption bands and giving rise to sphalerite’s orange, red, yellow, and green colors [25]. Optical absorption spectra of tetrahedral Fe^{2+} are reported by [18–20]. As another principal agent of sphalerite coloring, Co^{2+} in the tetrahedral Zn sites can be considered, which, even in small amounts (80 ppm), can cause the green color of sphalerite [14]. However, studied sphalerites from Slovakia have almost negligible amounts of Co (5–17 ppm). On the other hand, Cd instead of Co has more significant concentrations, even more than Fe in some samples. However, Cd with an

electronic configuration of $[\text{Kr}]4d^{10}$, similarly to Zn, has fully occupied d orbitals; therefore, no electron transitions can be expected in the visual region of the spectrum. Consequently, the bands between 669 and 743 nm can be very likely assigned to crystal-field bands of Fe^{2+} exclusively.

The black color of the sphalerite D sample is a matter of interest because of the similarity in absorption spectra with olive-green colored sphalerite (Figure 3). After disassembling the black sphalerite cluster into individual crystals, it turned out that the color of these crystals is very similar to olive green (Figure 3), which would explain the similarity of the optical spectrum of black and olive-green sphalerite. The black coloring could be caused by slightly higher concentrations of Fe (0.46 wt.%, 0.008 *apfu*, Table 1), the significantly smaller size of individual crystals in the aggregate reducing macroscopic transparency, and/or the presence of submicroscopic inclusions, which, however, were not observed even in the back-scattered electron images of the studied sample.

7. Conclusions

Gem-quality sphalerite from Slovakia was overlooked for a long time because it was considered to be only a zinc ore. Sphalerite from the Terézia and Rozália veins in the Banská Štiavnica ore district has relatively low content of Cd and Fe, which are substituting for Zn with the Cd/Fe ratio decreasing from 2.82–2.85 in the yellow sample to 0.42 in the black sample. LA-ICP-MS showed that only Cd, Fe, and Mn has content above 20 ppm and Co and Cu vary between 2 and 17 ppm. The optical absorption spectra exhibit absorption between 644 and 740 nm with three bands at 669–671, 698–702, and 732–743 nm, weaker absorption bands at 858–894 nm in the NIR region, the bands between 669 and 743 cm^{-1} which can be assigned to crystal-field bands of Fe^{2+} , and the absorption edge starting at about 600 nm to the UV region. Minimal absorption is in the yellow-red region resulting in yellowish-orange and orange-red colors. More pronounced absorption in the red region for olive-green sphalerite explains the shift to greenish hues. In black sphalerite, the absorption pattern is similar to the olive-green sphalerite. The black color could be caused by slightly higher Fe content and/or smaller grain size in the aggregate reducing macroscopic transparency. The gemologically interesting properties of sphalerite from the Banská Štiavnica area likely result from low Fe content connected with a relatively low temperature of fluids during sphalerite crystallization.

Author Contributions: Concept of study, J.F. and P.B.; field research and sample collection, P.S.; sample preparation, Z.P. and P.S.; methodology, P.B., J.F., O.R., J.Š., L.I., R.Š. and T.V.; formal investigation, P.B., J.F., J.Š. and L.I.; compilation and writing of the manuscript, P.B., J.F. and O.R.; review and editing of the manuscript, J.F., P.B. and O.R. All authors have read and agreed to the published version of the manuscript.

Funding: This research was funded by the Slovak Research and Development Agency under Contract number APVV-18-0065 and the Ministry of Education of Slovak Republic grant agency under contract KEGA 026UKF-4/2021.

Data Availability Statement: The data presented in this study are all available in the article.

Acknowledgments: We thank the editor and reviewers for their detailed reviews, which improved the quality of our work.

Conflicts of Interest: The authors declare no conflict of interest.

References

1. Cook, N.J.; Ciobanu, C.L.; Pring, A.; Skinner, W.; Shimizu, M.; Danyushevsky, L.; Saini-Eidukat, B.; Melcher, F. Trace and minor elements in sphalerite: A LA-ICPMS study. *Geochim. Cosmochim. Acta* **2009**, *73*, 4761–4791. [[CrossRef](#)]
2. Hurlbut, J.C.S.; Kammerling, R.C. *Gemology*; Wiley-Interscience: New York, NY, USA, 1991; pp. 1–337.
3. Ďud'a, R.; Ozdín, D. *Minerály Slovenska*; Granit: Prague, Czech Republic, 2012; pp. 1–480.
4. Velasco, F.; Herrero, J.M.; Yusta, I.; Alonso, J.A.; Seebold, I.; Leach, D. Geology and geochemistry of the Reocín zinc-lead deposit, Basque-Cantabrian Basin, Northern Spain. *Econ. Geol.* **2003**, *98*, 1371–1396. [[CrossRef](#)]
5. Wight, W. The Gems of Mont Saint-Hilaire, Quebec, Canada. *J. Gemmol.* **1996**, *25*, 24–44. [[CrossRef](#)]

6. Sainz De Baranda, B.; Garcia Garcia, G. The Picos de Europa lead-zinc deposits, Spain. *Mineral. Rec.* **1996**, *27*, 177–188.
7. Smith, A.E.; Pressler, C.D. A 1946 Find of Gem Sphalerite Crystals at the Balmat Zinc Mine, St. Lawrence County, New York. *Rocks Miner.* **1998**, *73*, 404–408. [[CrossRef](#)]
8. Muntyan, B.L. Colorado Sphalerite. *Rocks Miner.* **1999**, *74*, 220–235. [[CrossRef](#)]
9. Cook, R.B. Connoisseur's Choice: Sphalerite, Eagle Mine, Gilman, Eagle County, Colorado. *Rocks Miner.* **2003**, *78*, 330–334. [[CrossRef](#)]
10. Panczner, W.D. Important Mining Districts. In *Minerals of Mexico*; Springer: Berlin/Heidelberg, Germany, 1987; pp. 1–49.
11. Bonev, I.K.; Kouzmanov, K. Fluid inclusions in sphalerite as negative crystals: A case study. *Eur. J. Mineral.* **2002**, *14*, 607–620. [[CrossRef](#)]
12. Breskovska, V.; Tarkian, M. Mineralogy and fluid inclusion study of polymetallic veins in the Madjarovo ore field, Eastern Rhodope, Bulgaria. *Mineral. Petrol.* **1993**, *49*, 103–118. [[CrossRef](#)]
13. Vassileva, R.D.; Bonev, I.K.; Marchev, P.; Atanassova, R. 2-1: Pb-Zn deposits in the Madan ore field, South Bulgaria: Madan District: Lat. 41°30' N, Long. 24°56' E. *Ore Geol. Rev.* **2005**, *27*, 90–91. [[CrossRef](#)]
14. Rager, H.; Amthauer, G.; Bernroider, M. Colour, crystal chemistry, and mineral association of a green sphalerite from Steinperf, Dill syncline, FRG. *Eur. J. Mineral.* **1996**, *8*, 1191–1198. [[CrossRef](#)]
15. Ye, L.; Cook, N.J.; Ciobanu, C.L.; Yuping, L.; Qian, Z.; Tiegeng, L.; Wei, G.; Yulong, Y.; Danyushevskiy, L. Trace and minor elements in sphalerite from base metal deposits in South China: A LA-ICPMS study. *Ore Geol. Rev.* **2011**, *39*, 188–217. [[CrossRef](#)]
16. Wen, H.; Zhu, C.; Zhang, Y.; Cloquet, C.; Fan, H.; Fu, S. Zn/Cd ratios and cadmium isotope evidence for the classification of lead-zinc deposits. *Sci. Rep.* **2016**, *6*, 25273. [[CrossRef](#)] [[PubMed](#)]
17. Liu, S.; Zhang, Y.; Ai, G.; Xue, X.; Li, H.; Shah, S.A.; Wang, N.; Chen, X. LA-ICP-MS trace element geochemistry of sphalerite: Metallogenic constraints on the Qingshuitang Pb–Zn deposit in the Qinhang Ore Belt, South China. *Ore Geol. Rev.* **2022**, *141*, 104659. [[CrossRef](#)]
18. Slack, G.A.; Ham, F.S.; Chrenko, R.M. Optical absorption of tetrahedral Fe²⁺ (3d⁶) in cubic ZnS, CdTe, and MgAl₂O₄. *Phys. Rev.* **1966**, *152*, 376–402. [[CrossRef](#)]
19. Low, W.; Weger, M. Paramagnetic resonance and optical spectra of divalent iron in cubic fields. II. Experimental results. *Phys. Rev.* **1960**, *118*, 1130. [[CrossRef](#)]
20. Manning, P.G. Absorption spectra of Fe (III) in octahedral sites in sphalerite. *Can. Mineral.* **1967**, *9*, 57–64.
21. Schneider, J.; Kirby, R.D. Raman scattering from ZnS polytypes. *Phys. Rev. B* **1972**, *6*, 1290–1294. [[CrossRef](#)]
22. Hope, G.A.; Woods, R.; Munce, C.G. Raman microprobe mineral identification. *Miner. Eng.* **2001**, *14*, 1565–1577. [[CrossRef](#)]
23. Couture-Mathieu, L.; Mathieu, J.P. Raman spectra of ZnS. *Comptes Rendus Geosci.* **1953**, *236*, 371–385.
24. Nilsen, W.G. Raman spectrum of cubic ZnS. *Phys. Rev.* **1969**, *182*, 833.
25. Wincott, P.L.; Vaughan, D.J. Spectroscopic studies of sulfides. *Sulfide Mineral. Geochemistry* **2018**, *61*, 181. [[CrossRef](#)]
26. Ozdín, D.; Krejsek, Š. Famous mineral localities: Banská Štiavnica (Schemnitz, Selmečbánya), Slovak Republic. *Min Rec* **2016**, *47*, 254–318.
27. Born, I. *Lithophylacium Bornianum Sive Index Fossilium, Quae Collegit, et in Classes ac Ordines Disposuit*; Wolfgangum Gerle: Prague, Czech Republic, 1772; pp. 1–162.
28. Števkó, M. Nové nálezy minerálov na rudných žilách v Hodruši-Hámroch. *Minerál* **2015**, *23*, 422–434.
29. Konečný, V.; Lexa, J. Stavba a vývoj štiavnického stratovulkánu. *Miner. Slov.* **2001**, *33*, 179–196.
30. Lexa, J. Metalogenéza štiavnického stratovulkánu. *Miner. Slov.* **2001**, *33*, 203–214.
31. Lexa, J.; Štohl, J.; Konečný, V. The Banská Štiavnica ore district: Relationship between metallogenetic processes and the geological evolution of a stratovolcano. *Miner. Depos.* **1999**, *34*, 639–654. [[CrossRef](#)]
32. Fridrichová, J.; Bačík, P.; Štubňa, J.; Illášová, L. Sphalerite from Slovakia. *J. Gemmol.* **2020**, *37*, 12–13. [[CrossRef](#)]
33. Shannon, R.D. Revised effective ionic radii and systematic studies of interatomic distances in halides and chalcogenides. *Acta Crystallogr. Sect. A* **1976**, *32*, 751–767. [[CrossRef](#)]
34. Xuexin, S. Minor elements and ore genesis of the Fankou lead-zinc deposit, China. *Miner. Depos.* **1984**, *19*, 95–104.
35. Hofmann, C.; Henn, U. Grune Sphalerite aus Zaire. *Zeitschrift Dtsch. Gemmol. Gesellschaft* **1984**, *33*, 72–74.
36. Intiomale, M.M.; Oosterbosch, R. Géologie et géochimie du gisement de Kipushi, Zaïre. *Ann. Société Géologique Belg.* **1974**, *123*–164.

Disclaimer/Publisher's Note: The statements, opinions and data contained in all publications are solely those of the individual author(s) and contributor(s) and not of MDPI and/or the editor(s). MDPI and/or the editor(s) disclaim responsibility for any injury to people or property resulting from any ideas, methods, instructions or products referred to in the content.